

# Study of Age, Metallicity and Extra-Tidal region of a Globular Cluster NGC 4147

Group 6

Observational Astronomy Lab

Department of Physics and Astrophysics,  
University of Delhi

April 15, 2025



# Outline

- 1 Introduction and Background
- 2 Motivation
- 3 Data and Methodology
- 4 Data Analysis
- 5 Results and Conclusion



# Defining Globular Clusters

## What are globular clusters?

- Globular clusters are dense, metal-poor, spherical groups of old stars orbiting the Milky Way
- They help trace the Galaxy's formation and test stellar evolution theories



**Figure:** NGC 4147 is located about 60,000 light-years from Earth in the northern constellation of Coma Berenices.  
Credit: ESA/Hubble & NASA, T. Sohn et al.



# Defining Globular Clusters

- The Milky Way has a bulge, spiral disk, and an extended halo
- Globular clusters reside in the halo, distributed spherically around the Galactic center

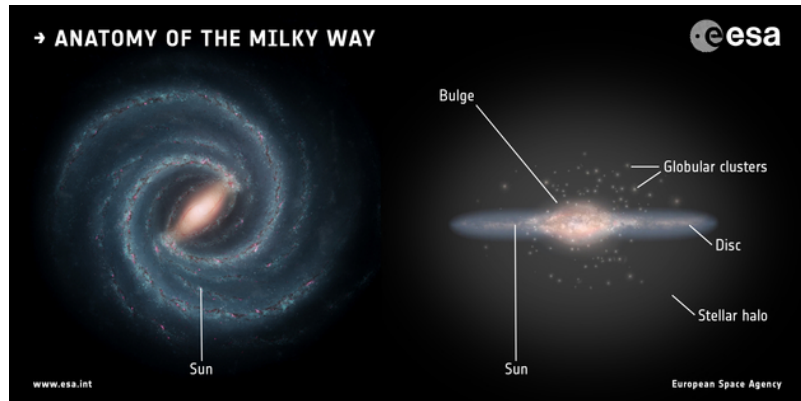


**Figure:** Credit: Left: NASA/JPL-Caltech; right: ESA; layout: ESA/ATG medialab



# Understanding Color-Magnitude Diagram (CMD)

- The CMD is an observational version of the Hertzsprung–Russell diagram, using apparent magnitude and color instead of luminosity and temperature
- CMDs are especially useful when luminosity or temperature cannot be measured directly
- Color (e.g.,  $B_p - R_p$ ) acts as a proxy for temperature, while magnitude (e.g.,  $G$ ) relates to brightness.
- The Gaia satellite provides photometry in  $G$ ,  $B_p$ , and  $R_p$  bands, allowing astronomers to build CMDs for millions of stars.

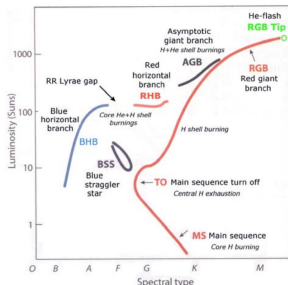
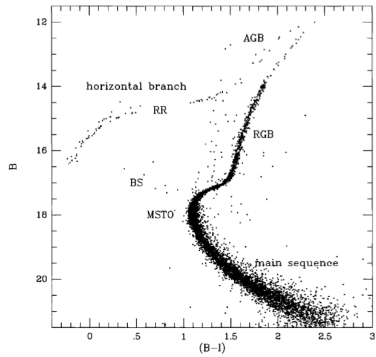


Figure: Color-magnitude diagram for a typical globular cluster. [1]



# Understanding Color-Magnitude Diagram (CMD)

- It reveals stellar evolutionary features—main sequence, red giant branch, and horizontal branch—especially in globular clusters.
- The main sequence turn-off point helps estimate a cluster's age; CMDs also assist in identifying cluster members and estimating distance.



**Figure:** CMD showing the main sequence, turn-off point (MSTO), red giant branch (RGB), asymptotic giant branch (AGB), RR Lyrae gap, horizontal branch, and blue stragglers (BS) in a globular cluster [2].

# Main Sequence

- **Structure & Turn-off Point:**

Well-defined band of hydrogen-burning stars.

Turn-off point indicates age — older clusters have fainter, redder turn-offs ( $\sim 0.8 M_{\odot}$ , age  $\sim 12\text{--}15$  Gyr [3]).

- **Metallicity & Mass Limit:**

Higher metallicity  $\rightarrow$  redder, fainter main sequence.

Stars below  $\sim 0.08 M_{\odot}$  can't sustain hydrogen fusion and become brown dwarfs [4].

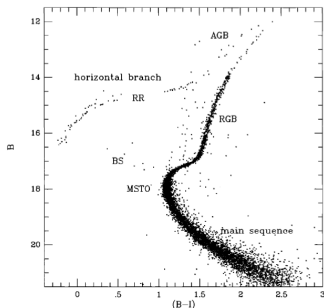


**Figure:** CMD showing the main sequence, turn-off point (MSTO), red giant branch (RGB), asymptotic giant branch (AGB), RR Lyrae gap, horizontal branch, and blue stragglers (BS) in a globular cluster [2].



# Red Giant Branch

- **Evolution:** Stars move from the subgiant region to brighter, redder colors as they exhaust hydrogen.
- **Helium Flash:** The RGB ends with the ignition of helium, marking the start of the horizontal branch.
- **Metallicity:** Metal-rich clusters have redder, shallower RGBs, while metal-poor clusters have bluer, steeper branches.

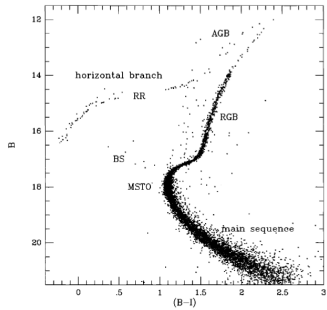


**Figure:** CMD showing the main sequence, turn-off point (MSTO), red giant branch (RGB), asymptotic giant branch (AGB), RR Lyrae gap, horizontal branch, and blue stragglers (BS) in a globular cluster [2].

# Horizontal Branch

- **HB Evolution:** Stars burn helium in their cores, forming a horizontal sequence in the CMD with similar luminosity and bluer colors.
- **RR Lyrae Stars:** Metal-poor stars serve as excellent distance indicators.
- **Metallicity & Age:** Metal-rich clusters have redder HBs, metal-poor clusters show bluer, extended HBs.

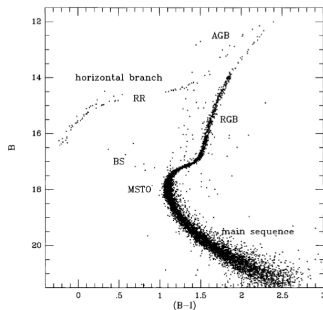


**Figure:** CMD showing the main sequence, turn-off point (MSTO), red giant branch (RGB), asymptotic giant branch (AGB), RR Lyrae gap, horizontal branch, and blue stragglers (BS) in a globular cluster [2].

# Asymptotic Giant Branch

- **AGB Evolution:** AGB stars ( $0.88M_{\odot}$ ) evolve after helium exhaustion, with shell burning around a carbon-oxygen core.
- **End of AGB:** Mass loss ejects the stellar envelope, leaving a post-AGB star that evolves into a white dwarf.

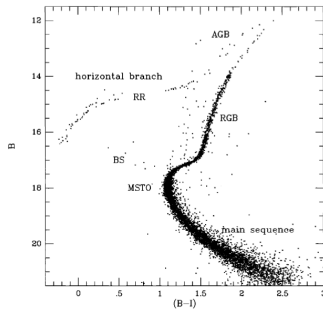


**Figure:** CMD showing the main sequence, turn-off point (MSTO), red giant branch (RGB), asymptotic giant branch (AGB), RR Lyrae gap, horizontal branch, and blue stragglers (BS) in a globular cluster [2].



# Blue Stragglers

- **Unusual Position:** Blue stragglers extend the main sequence beyond the turn-off, appearing hotter and more luminous than expected for their age.
- **Formation Mechanisms:** They form through mass transfer in binary systems or stellar collisions, with the dominant process depending on the environment.

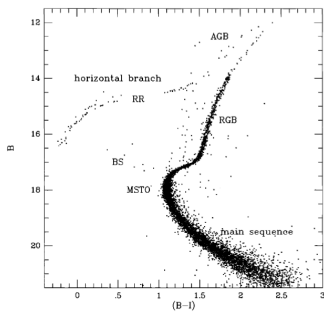


**Figure:** CMD showing the main sequence, turn-off point (MSTO), red giant branch (RGB), asymptotic giant branch (AGB), RR Lyrae gap, horizontal branch, and blue stragglers (BS) in a globular cluster [2].



# Motivation

- **NGC 4147** is an *old, metal-poor, and isolated* globular cluster in Coma Berenices.
- Located about **18.5 kpc** from the Sun at a galactic latitude of  $77.2^\circ$ .
- Its position makes it a candidate for its association with the **Sagittarius tidal stream** suggesting it may have been captured by the **Milky Way** after it's separation from the **Sagittarius Dwarf Spheroidal Galaxy**.

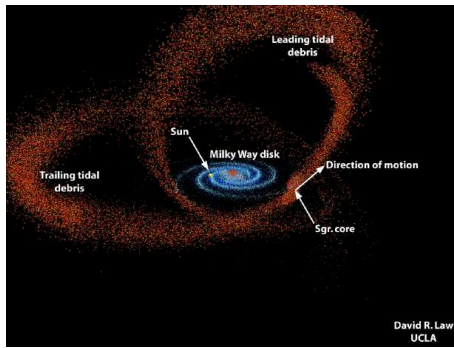


Figure: Credit: David R Law, UCLA



# Motivation

- We aim to study the age, metallicity, and extra-tidal region of **NGC 4147** using Gaia DR3 data.
- Identify **extra-tidal candidates** based on cluster and stellar proper motions, and their positions on the color-magnitude diagram.
- Analyze the spatial distribution of these stars to understand the cluster's dynamical history within the Milky Way.



# Data Acquisition

## Obtaining the raw data sample

- The data used in this study has been obtained from Gaia Data Release 3 (DR3).
- Key parameters such as right ascension, declination, proper motion and its associated uncertainties, as well as photometric information (e.g., color and magnitude) for each star in the cluster were retrieved using the Astronomical Data Query Language (ADQL).

## Cleaning the data-sets

- To select astrometrically well-behaved sources, we applied the criteria as recommended in the data release documentation and literature [5].
- We obtained a total of **2389** stars after this process.



# Data Acquisition

S.No	$\alpha$ (RA)	$\delta$ (Dec)	$\mu_\alpha \cos \delta$	$\mu_\delta$	$\sigma_{\mu_\alpha \cos \delta}$	$\sigma_{\mu_\delta}$
1	182.549859	18.539132	-2.066131	-0.994648	1.095702	0.872899
2	182.539023	18.533168	-2.165506	-2.731644	0.854342	0.599843
3	182.556507	18.556774	-1.910701	-2.036851	0.615011	0.467600
4	182.485128	18.570416	-1.926746	-1.412548	0.729234	0.675337
5	182.472899	18.572690	1.207729	-2.082758	1.248144	0.811114

**Table:** Proper motion and positional data for 5 stars in NGC 4147 extracted from Gaia DR3.



# Data Reduction

*We began our analysis by selecting only those stars which seemed to be the cluster members.*

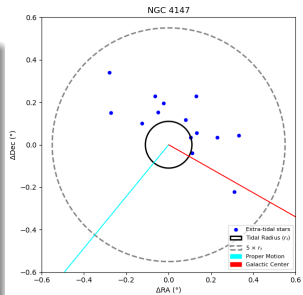
To obtain these possible members, we selected stars based on the following criteria:

- ① **Proper motion of the star** consistent with the **proper motion of the cluster**.
- ② Consistent with the selection based on the **membership probabilities**.
- ③ Location in the **color-magnitude diagram** (CMD) consistent with the **CMD** of the cluster.



# Data Reduction

- Only stars that met the mentioned criteria were considered **probable members** of the cluster.
- These criteria were applied to all stars located within a radius extending up to **five** times the **tidal radius ( $r_t$ )** of the cluster [6].
- Stars positioned between  $r_t$  and  $5r_t$  from the center of the cluster were identified as **extra-tidal candidates** for further analysis.
- For this study, the adopted value of  $r_t$  is **6.6 arcmin** [7].



A detailed explanation of the implementation of these selection conditions will be explained in the coming slides.



# Proper Motion Selection

**Proper motion** is the astrometric measure of the observed changes in the apparent places of stars or other celestial objects in the sky, as seen from the center of mass of the Solar System, compared to the abstract background of the more distant stars.

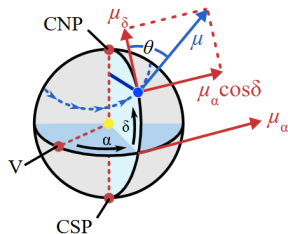


**Figure:** Representation of pmra and pmdec on a celestial sphere. [8].

For NGC 4147 [5]:

- RA:  $182.5263^\circ$ , DEC:  $18.542^\circ$
- $\overline{\mu_\alpha \cos \delta} = -1.71 \text{ mas yr}^{-1}$ ,  $\overline{\mu_\delta} = -2.08 \text{ mas yr}^{-1}$
- $\sigma_{\mu_\alpha \cos \delta} = 0.21 \text{ mas yr}^{-1}$ ,  $\sigma_{\mu_\delta} = 0.19 \text{ mas yr}^{-1}$

# Proper Motion Selection

Now, in order to obtain likely cluster members, we cut the sample at  $PM \pm 3\sigma$  to only select stars as our cluster members:

$$\sqrt{(\mu_\alpha \cos \delta - \bar{\mu}_\alpha \cos \delta)^2 + (\mu_\delta - \bar{\mu}_\delta)^2} < 3\sqrt{\sigma_{\mu_\alpha \cos \delta}^2 + \sigma_{\mu_\delta}^2} \quad (1)$$

We get a total of **474 stars** (**411** = cluster stars, **63** = extra-tidal stars)

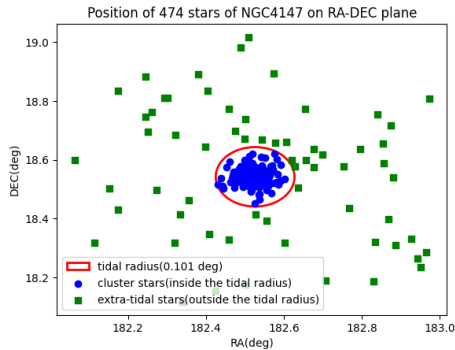


**Figure:** Position of stars on RA-DEC plane, compatible with proper motion of cluster NGC4147.



# Membership Probability

**Membership probability** refers to the likelihood that a star near a globular cluster belongs to it, rather than being a field star.

We used the **maximum likelihood method**, based on a Bayesian approach from [9, 10], applied to stars selected by proper motion.

Probability Density Functions (p.d.f.):

Cluster stars:

$$\phi_c^\nu = \frac{1}{2\pi\sqrt{(\sigma_c^2 + \epsilon_{xi}^2)(\sigma_c^2 + \epsilon_{yi}^2)}} \times \exp\left(-\frac{1}{2}\left[\frac{(\mu_{xi} - \mu_{xc})^2}{\sigma_c^2 + \epsilon_{xi}^2} + \frac{(\mu_{yi} - \mu_{yc})^2}{\sigma_c^2 + \epsilon_{yi}^2}\right]\right) \quad (2)$$

Field stars (Stars that lie outside the tidal radius):

$$\begin{aligned} \phi_f^\nu = & \frac{1}{2\pi\sqrt{(1-\gamma^2)(\sigma_{xf}^2 + \epsilon_{xi}^2)(\sigma_{yf}^2 + \epsilon_{yi}^2)}} \\ & \times \exp\left(-\frac{1}{2(1-\gamma^2)}\left[\frac{(\mu_{xi} - \mu_{xf})^2}{\sigma_{xf}^2 + \epsilon_{xi}^2} - \frac{2\gamma(\mu_{xi} - \mu_{xf})(\mu_{yi} - \mu_{yf})}{\sqrt{(\sigma_{xf}^2 + \epsilon_{xi}^2)(\sigma_{yf}^2 + \epsilon_{yi}^2)}} + \frac{(\mu_{yi} - \mu_{yf})^2}{\sigma_{yf}^2 + \epsilon_{yi}^2}\right]\right) \end{aligned} \quad (3)$$

$\gamma$  is the correlation coefficient defined as:

$$\gamma = \frac{(\mu_{xi} - \mu_{xf})(\mu_{yi} - \mu_{yf})}{\sigma_{xf}\sigma_{yf}} \quad (4)$$



# Membership Probability

Intrinsic dispersion of the cluster's proper motion:

$$\sigma_c = \frac{\sigma_v}{R_\odot} \quad (5)$$

$\sigma_v$  (central velocity dispersion) = 0.00000265723093 pc yr<sup>-1</sup>

$R_\odot$  (distance of the cluster from the sun) = 19300 pc taken from [11].

Using Gaussian fit, the field parameters calculated are :

$$\mu_{xf} = -1.67 \text{ mas yr}^{-1}, \quad \sigma_{xf} = 0.56 \text{ mas yr}^{-1}$$

$$\mu_{yf} = -2.19 \text{ mas yr}^{-1}, \quad \sigma_{yf} = 0.36 \text{ mas yr}^{-1}$$

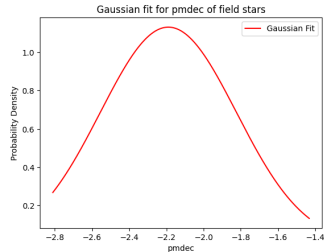
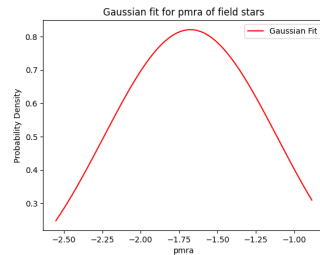


Figure: Gaussian fit for pmra ( $\mu_\alpha \cos \delta$ ) and pmdec ( $\mu_\delta$ ) of field stars.



# Membership Probability

The membership probability for the  $i$ th star is:

$$P(i) = \frac{n_c \phi_c^\nu}{\phi^\nu} \quad (6)$$

The total distribution function ( $\phi^\nu$ ) is:

$$\phi^\nu = n_c \phi_c^\nu + n_f \phi_f^\nu \quad (7)$$

Here,  $n_c$  and  $n_f$  are the normalized number of cluster stars and extra-tidal stars. These values are:  $n_c = 0.867$ ,  $n_f = 0.133$  which satisfy  $n_c + n_f = 1$ .

We retained **440** stars (**411** cluster stars and **29** extra-tidal stars) for further analysis.

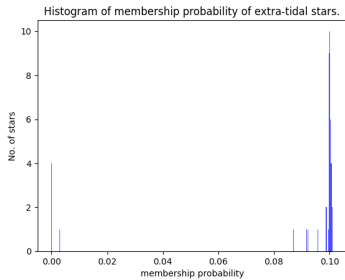


**Figure:** Histogram of membership probability for extra-tidal stars, showing most stars have  $P(i)$  around 10%.



# Color-Magnitude Diagram

For **Extinction Correction**, the equation [12] used is,

$$G_0 = G - R_G \times 3.1 \times E(B - V) \quad (8)$$

$$(G_{BP} - G_{RP})_0 = (G_{BP} - G_{RP}) - (R_{BP} - R_{RP}) \times 3.1 \times E(B - V) \quad (9)$$

where,

$$R_G = 2.726$$

$$R_{BP} = 3.310$$

$$R_{RP} = 2.009$$

$$E(B - V) = 0.02$$

The coefficients for Gaia band passes were obtained from the [13] & the E(B-V) value from [11].

S No.	G	$G_{BP}$	$G_{RP}$	$G_{BP} - G_{RP}$
1	20.225628	20.438187	19.793797	0.644390
2	19.926857	20.224590	19.616734	0.607857
3	19.810244	20.088234	19.513187	0.575047
4	21.047251	20.802969	20.768568	0.034401
5	20.858648	20.655558	20.890247	-0.234690

**Table:** Color-Magnitude data for five stars in NGC 4147 obtained from Gaia DR3.



# Color-Magnitude Diagram

- In the CMD of NGC 4147, **no Main Sequence** is left.
- It shows a **red giant branch** with a **red turn-off point**, indicating that the cluster is very **old**.
- **Gaps** along the **horizontal branch** may suggest the presence of **RR Lyrae variables**.

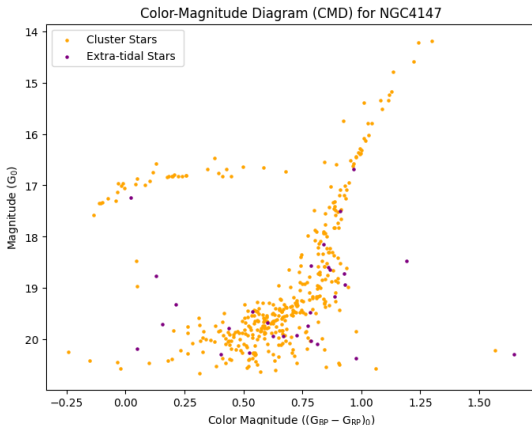


Figure: Color Magnitude Diagram for NGC 4147.



# Isochrone Fitting

To estimate the **age** and **metallicity** of NGC 4147 and to select the most likely **extra-tidal candidates**, we performed **Isochrone Fitting** using models from the PARSEC stellar evolution database [14].

Isochrone fitting involves comparing theoretical stellar evolution tracks with observed CMDs. We selected 6 isochrone models from PARSEC database each with varying:

- Age (in  $\log(\text{Age}/\text{yr})$ )
- Metallicity ( $[\text{Fe}/\text{H}]$  in dex)

Each isochrone represents a population of stars with specific age and chemical composition.

**PARSEC** models provide apparent magnitudes in Gaia G,  $G_{BP}$ , and  $G_{RP}$  bands, which will be further corrected for extinction and distance modulus.



# Isochrone Fitting

## Fitting Methodology

Each isochrone was tested against the observed CMD of NGC 4147 by applying a trial distance modulus (DM) and minimizing the average squared distance between isochrone points and cluster stars in CMD space:

- 1 Correct Gaia magnitudes for extinction and apply a trial distance modulus:

$$G_{\text{fit}} = G_0 + DM \quad (10)$$

- 2 Define a cost function using the average squared distance between isochrone and observed points:

$$\chi^2 = \frac{1}{N} \sum_i \min_j [(c_i - c_j)^2 + (m_i - m_j)^2] \quad (11)$$

where  $(c_i, m_i)$  are isochrone color-magnitude pairs and  $(c_j, m_j)$  are observed stars.

- 3 Alternatively,

$$\chi^2 = \min \left[ (G_0^{\text{obs}} - (G_0^{\text{iso}} + DM))^2 + ((BP - RP)_0^{\text{obs}} - (BP - RP)_0^{\text{iso}})^2 \right] \quad (12)$$

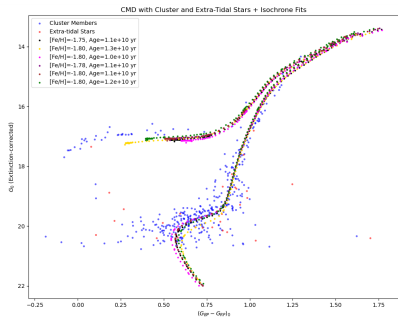
- 4 Use `scipy.optimize.minimize` from SciPy [15] to find the DM that minimizes  $\chi^2$ .

The isochrone with the lowest  $\chi^2$  is taken as the best fit.



# Isochrone Fitting

## Isochrone Fits



## Best Fit Isochrone

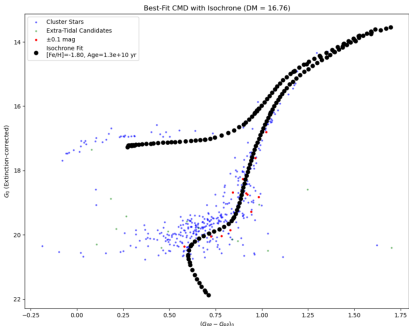


**Figure:** On the left we have CMD of NGC 4147 with several PARSEC isochrone models of different ages and metallicities overplotted and on the right we have Best-fit isochrone model selected by minimizing the average distance in CMD space.



# Isochrone Fitting

## Identifying extra-tidal candidates

- The already selected **29** extra-tidal stars are compared with the best-fit isochrone, and those within  $\pm 0.1$  mag in both color and magnitude are considered as the most likely extra-tidal stars of the cluster.
- Using this method, a total of **14** extra-tidal stars were found to lie along the best-fit isochrone.

## Estimating Age and Metallicity

The best-fitting isochrone directly provides estimates of the cluster's:

- **Age**, inferred from the position of the main sequence turnoff and subgiant branch. From the best-fit model, the age of NGC 4147 is estimated to be  $(1.3 \pm 0.2) \times 10^{10}$  years, compared to [16].
- **Metallicity**, inferred from the slope and shape of the red giant branch and other CMD features. The corresponding metallicity is found to be  $[\text{Fe}/\text{H}] = -1.8$  dex, which is consistent with the results in [16].



# Density Plot

- The density maps were created using the **kernel density estimator** (KDE) routine of the `scipy` module [15].
- $\Delta RA$  is the difference between the RA of the extra-tidal star and the RA of the cluster, the same as for  $\Delta Dec$ .
- The contour lines represent the iso-density regions with a constant number of stars per square degree [5].

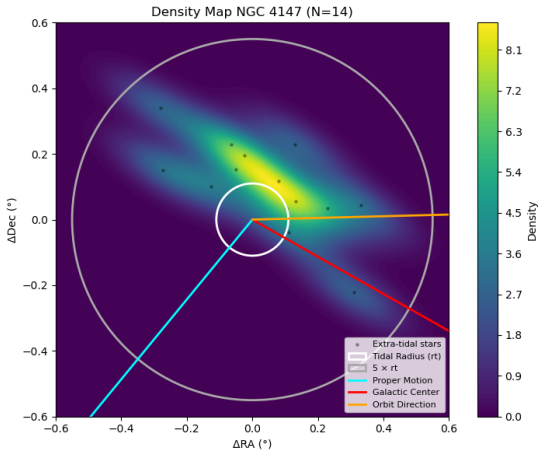


**Figure:** Density Map of the selected extra-tidal candidates (black dots), along with the PM (blue) of the cluster,  $r_t$  (white),  $5r_t$  (dark grey), the direction of the galactic center (red line) and the orbit of the cluster in the future(orange line).



# Orbit of the Cluster

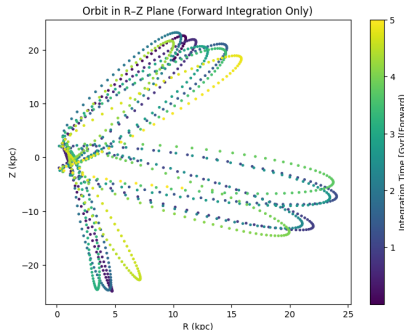
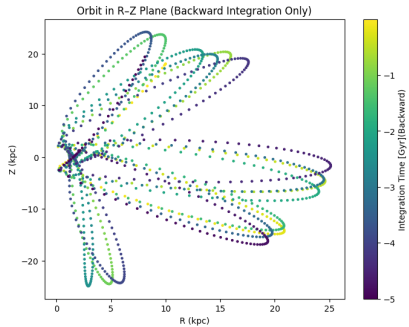


**Figure:** Orbit of NGC 4147 in the  $R$ - $Z$  plane. The pair shows backward and forward integrations over 5 Gyr. The plots were obtained using Gravpot16 Web Interface [17].



# Orbit of the Cluster

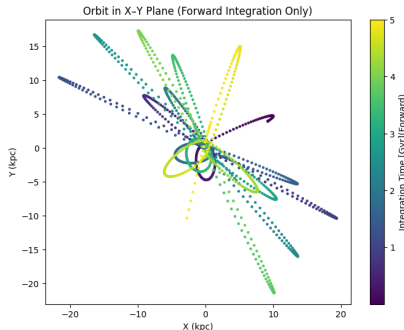
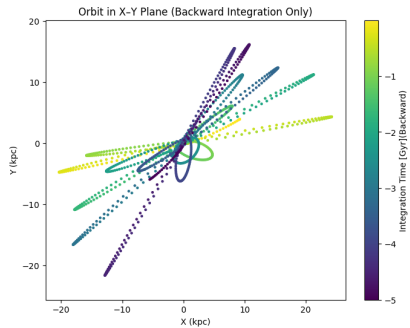


**Figure:** Orbit of NGC 4147 in the X-Y plane. The pair shows backward and forward integrations over 5 Gyr. The plots were obtained using Gravpot16 Web Interface [17].



# Results and Conclusion

- We estimated the **age** and **metallicity** of NGC 4147 to be:

- ①  $(1.3 \pm 0.2) \times 10^{10}$  years
- ② -1.8 dex

These values are based on CMD analysis and isochrone fitting, and are consistent with previous studies.

- For selecting **extra-tidal stars**, we began with **2389** stars. After applying proper motion and CMD-based selection criteria, we shortlisted **425** probable members.



## Results and Conclusion

- Among them, **14** stars were identified as the most likely **extra-tidal candidates**. This list may be incomplete, as some stars might have drifted beyond the  $5r_t$  region and were not captured in our selection.
- The density map reveals an overdensity of candidates in the direction opposite to the cluster's proper motion. Combined with the orbital analysis, this suggests that NGC 4147 has undergone repeated disk and/or bulge crossings.
- These interactions likely caused tidal stripping of stars from the cluster's outskirts, leading to the formation of extended extra-tidal features.



**Thank you for your attention**



# Bibliography I



[George Djorgovski.](#)

Extragalactic astronomy & cosmology: Globular clusters, 2005.  
Lecture notes, Caltech Astronomy AY20 course.



[K. M. Ashman and S. E. Zepf.](#)

*Globular Cluster Systems.*  
Cambridge University Press, 1998.



[P. B. Stetson, D. A. VandenBerg, and M. Bolte.](#)

The ages of globular clusters in the halo of the galaxy.  
*Publications of the Astronomical Society of the Pacific*, 108(723):560–578, 1996.



[B. W. Carroll and D. A. Ostlie.](#)

*An Introduction to Modern Astrophysics.*  
Cambridge University Press, 2017.



[Richa Kundu, Camila Navarrete, Luca Sbordone, Julio A. Carballo-Bello, José G. Fernández-Trincado, Dante Minniti, and Harinder P. Singh.](#)

Extra-tidal star candidates in globular clusters of the sagittarius dwarf spheroidal galaxy.  
*Astronomy & Astrophysics*, 665:A8, August 2022.



[Ivan King.](#)

The structure of star clusters. I. an empirical density law.  
, 67:471, October 1962.



[Julio A. Carballo-Bello, Antonio Sollima, David Martínez-Delgado, Berenice Pila-Díez, Ryan Leaman, Jürgen Fliri, Ricardo R. Muñoz, and Jesús M. Corral-Santana.](#)

A search for stellar tidal debris of defunct dwarf galaxies around globular clusters in the inner galactic halo.  
*Monthly Notices of the Royal Astronomical Society*, 445(3):2971–2993, October 2014.



# Bibliography II



Wikipedia contributors.

Ngc 4147.

[https://en.wikipedia.org/wiki/NGC\\_4147](https://en.wikipedia.org/wiki/NGC_4147), 2025.

Accessed: 2025-04-08.



D. P. Sariya, R. K. S. Yadav, and A. Bellini.

Proper motions and membership probabilities of stars in the region of globular cluster ngc 6809.

*Astronomy & Astrophysics*, 543:A87, 2012.



L. Balaguer-Núñez, C. Jordi, D. Galadí-Enríquez, and J. L. Zhao.

New membership determination and proper motions of ngc 1817. parametric and non-parametric approach.

*Astronomy & Astrophysics*, 426:819–826, 2004.



W. E. Harris.

A catalog of parameters for globular clusters in the milky way (2010 edition).

<https://www.physics.mcmaster.ca/~harris/mwgc.dat>, 1996.

AJ, 112, 1487. The catalog is periodically updated; use the 2010 edition.



Henri M.J. Boffin.

Colour-magnitude diagrams.

<https://www.eso.org/~hboffin/Teaching/CMD.html>, n.d.

Accessed: 2025-04-10.



L. Casagrande, J. Lin, A. D. Rains, F. Liu, S. Buder, J. Horner, M. Asplund, G. F. Lewis, S. L. Martell, T. Nordlander, D. Stello, Y.-S. Ting, R. A. Wittenmyer, J. Bland-Hawthorn, A. R. Casey, G. M. De Silva, V. D’Orazi, K. C. Freeman, M. R. Hayden, ..., and T. Zwitter.

The galah survey: Effective temperature calibration from the infrared flux method in the gaia system.

*Monthly Notices of the Royal Astronomical Society*, 507(2):2684–2696, 2021.



# Bibliography III



PARSEC, CMD Web Tool.

Cmd 3.8 - web interface.

<https://stev.oapd.inaf.it/cgi-bin/cmd>, 2025.



Pauli Virtanen, Ralf Gommers, Travis E. Oliphant, and et al.

SciPy 1.0: Fundamental algorithms for scientific computing in python.

*Nature Methods*, 17:261–272, 2020.



Ying-Hua Zhang, Jundan Nie, Hao Tian, and Chao Liu.

Assessing the association between the globular cluster ngc 4147 and the sagittarius dwarf galaxy.

*The Astronomical Journal*, 168(6):237, 2024.



J. G. Fernandez-Trincado, A. C. Robin, C. Reylé, and O. Valenzuela.

GravPot16: A Galactic potential model.

<https://gravpot.utmam.cnrs.fr/>, 2016.

Accessed: 2025-04-13.

